

High Efficiency Single Phase Transformerless Inverter for Grid Connected PV System

Komal P. Banne

PG Student [Power System], Dept. of EE, Bhivrabai Sawant College of Engineering and Research, Pune, India

ABSTRACT: This paper presents single-phase transformerless grid-connected inverter that utilizes superjunction MOSFETs to achieve high efficiency for photovoltaic applications. In proposed inverter due to the splitting structure of inductor avoids reverse-recovery issues for the main power switches. High-frequency pulse width modulation switching commutation and the grid zero crossing instants, improving the quality of the output ac-current and increasing the converter efficiency. Also due to two additional AC-sides switches conducting the currents during the freewheeling phases so that the photovoltaic array is decoupled from the grid. This reduces the high-frequency common-mode voltage leading to minimized ground loop leakage current. This Paper describes H5 & H6 transformerless inverter topology. Detail analysis of proposed transformerless inverter with operation modes, common-mode leakage current analysis and design consideration of the proposed transformerless inverter in MATLAB simulation model are presented.

KEYWORDS: Conventional H5 and H6 Transformerless Inverters, Proposed Transformerless Inverter, Ground leakage current analysis.

I. INTRODUCTION

Transformerless inverters are widely used in grid-tied photovoltaic (PV) generation systems, due to the benefits of achieving high efficiency and low cost. Various transformerless inverter topologies have been proposed to meet the safety requirement of leakage currents, when no transformer is used in a grid connected photovoltaic system, a galvanic connection between the grid and PV array exists. In these conditions, dangerous leakage currents (common-mode currents) can appear through the stray capacitance between the PV array and the ground. In order to avoid these leakage currents, different inverter topologies that generate no varying common-mode voltages have been proposed.

II. VARIOUS TRANSFORMERLESS TOPOLOGIES

In recent years, there have been quite a few new transformerless PV inverters topologies, which eliminate traditional line frequency transformers to achieve lower cost and higher efficiency, and maintain lower leakage current as well. One unipolar inverter topology, H5, as shown in Fig.1, solves the ground leakage current issue and uses hybrid MOSFET and IGBT devices to achieve high efficiency.

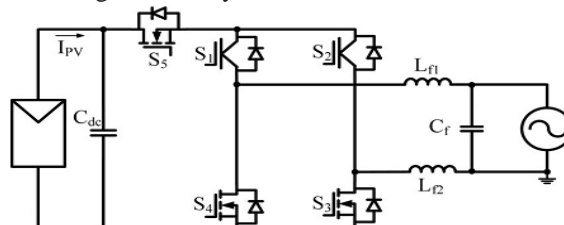


Fig.1. H5 Topology

This topology has high conduction losses due to the fact that the current must conduct through three switches in series during the active phase. Another disadvantage of the H5 is that the line-frequency switches S1 and S2 cannot utilize MOSFET devices because of the MOSFET body diode's slow reverse recovery. The slow reverse recovery of the MOSFET body diode can induce large turn-on losses, has a higher possibility of damage to the devices and leads to

International Journal of Advanced Research in Electrical, Electronics and Instrumentation Engineering

(An ISO 3297: 2007 Certified Organization)

Vol. 5, Issue 4, April 2016

EMI problems. Shoot-through issues associated with traditional full bridge PWM inverters remain in the H5 topology due to the fact that the three active switches are series-connected to the dc bus.

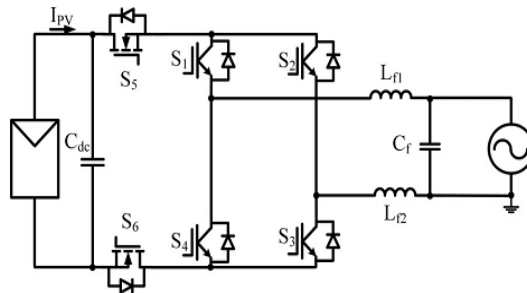


Fig.2. H6 Topology

H6 Topology uses MOSFETs to decrease the conduction loss of IGBTs in H5 topology, by splitting S5 of H5 topology into two MOSFETs i.e. S5 and S6 in series and operates them in high-frequency switching, S1–S4 in line grid line frequency switching. Uency switching, S1–S4 in line grid line frequency switching. Drawbacks of this inverter are higher conduction loss from four devices in conduction loop.

III. PROPOSED HIGH EFFICIENCY AND PV TRANSFORMERLESS INVERTER TOPOLOGY

The proposed transformerless PV inverter, which is composed of six MOSFETs switches (S1–S6), six diodes (D1–D6), and two split ac-coupled inductors $L1$ and $L2$ as shown in Fig.3. The diodes D1–D4 perform voltage clamping functions for active switches S1–S4. The ac-side switch pairs are composed of S5, D5 and S6, D6, respectively, which provide unidirectional current flow branches during the freewheeling phases decoupling the grid from the PV array and minimizing the CM leakage current. The proposed inverter topology divides the ac side into two independent units for positive and negative half cycle. In addition to the high efficiency and low leakage current features, the proposed transformerless inverter avoids shoot-through enhancing the reliability of the inverter.

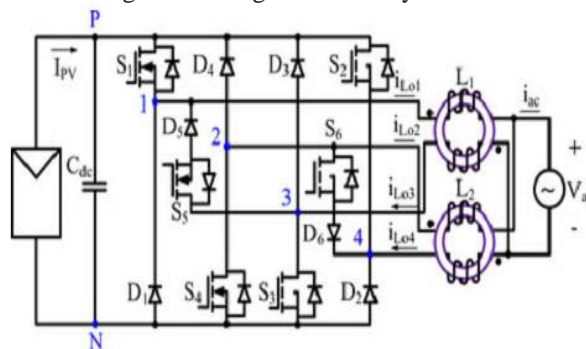


Fig.3. Proposed transformerless inverter

For proposed inverter, in the PWM scheme, when the reference signal $V_{control}$ is higher than zero, MOSFETs S1 and S3 are switched simultaneously in the PWM mode and S5 is kept on as a polarity selection switch in the half grid cycle; the gating signals G2, G4, and G6 are low and S2, S4, and S6 are inactive. Similarly, if the reference signal $-V_{control}$ is higher than zero, MOSFETs S2 and S4 are switched simultaneously in the PWM mode and S6 is on as a polarity selection switch in the grid cycle; the gating signals G1, G3, and G5 are low and S1, S3, and S5 are inactive.

International Journal of Advanced Research in Electrical, Electronics and Instrumentation Engineering

(An ISO 3297: 2007 Certified Organization)

Vol. 5, Issue 4, April 2016

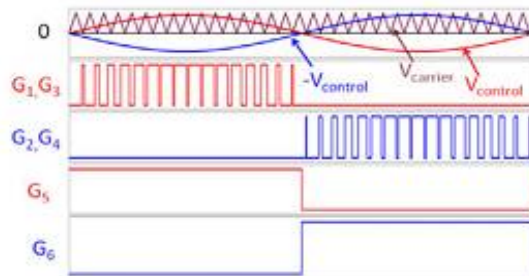


Fig.4 Gate signal of proposed transformerless inverter

The four operation stages of the proposed inverter are within one grid cycle. In the positive half-line grid cycle, the high-frequency switches S1 and S3 are modulated by the sinusoidal reference signal $V_{control}$ while S5 remains turned ON. When S1 and S3 are ON, diode D5 is reverse-biased, the inductor currents of i_{L1} and i_{L3} are equally charged, and energy is transferred from the dc source to the grid; when S1 and S3 are deactivated, the switch S5 and diode D5 provide the inductor current i_{L1} and i_{L3} a freewheeling path decoupling the PV panel from the grid to avoid the CM leakage current. Coupled-inductor L2 is inactive in the positive half-line grid cycle.

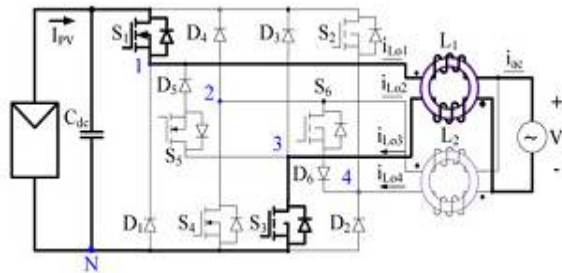


Fig.5 (a) Active stage of positive half cycle

Similarly, in the negative half cycle, S2 and S4 are switched at high frequency and S6 remains ON. Freewheeling occurs through S6 and D6.

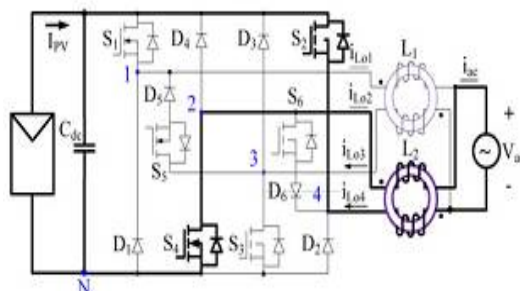


Fig.5 (b) Active stage of negative half cycle

Freewheeling occurs during positive half cycle through S5 & D5. Thus energy can be transferred from split case inductor to switch S5.

International Journal of Advanced Research in Electrical, Electronics and Instrumentation Engineering

(An ISO 3297: 2007 Certified Organization)

Vol. 5, Issue 4, April 2016

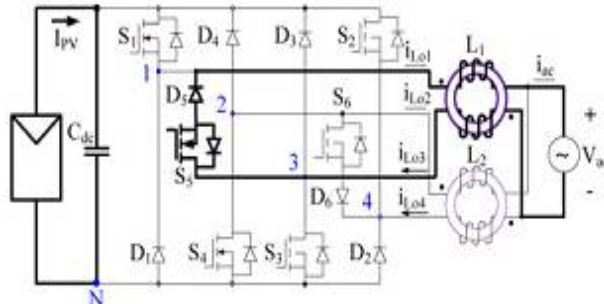


Fig.5 (c) Freewheeling stage of positive half cycle

During negative half cycle freewheeling occurs through S6 & D6. Thus energy can be transferred from another split case inductor to switch S6.

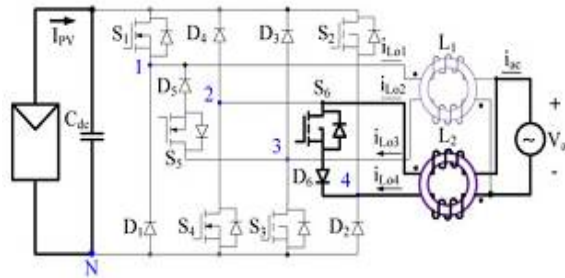


Fig.5 (d) Freewheeling stage of negative half cycle

IV. GROUND LOOP LEAKAGE CURRENT ANALYSIS FOR THE PROPOSED TRANSFORMERLESS INVERTER

A galvanic connection between the ground of the grid and the PV array exists in transformerless grid-connected PV systems. Large ground leakage currents may appear due to the high stray capacitance between the PV array and the ground. To analyze the ground loop leakage current, Figure shows a model with the phase output points 1, 2, 3, and 4 modeled as controlled voltage sources connected to the negative terminal of the dc bus.

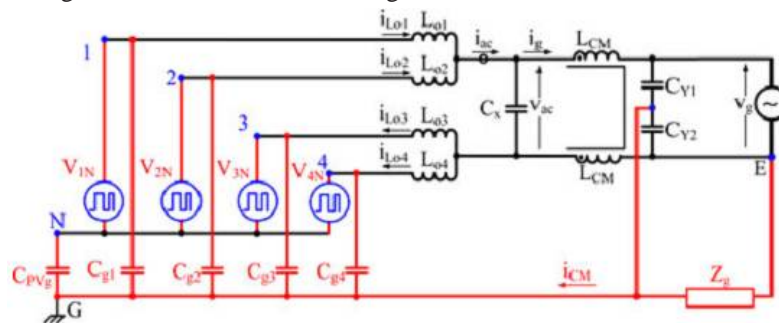


Fig.6 Leakage current analysis model

Fig.6 clearly shows the stray elements influencing the ground leakage current, which include:

- 1) The stray capacitance between PV array and ground C_{PVg} ;
- 2) Stray capacitances between the inverter devices and the ground $C_{g1} - C_{g4}$ and
- 3) The series impedance between the ground connection points of the inverter and the grid Z_g .

The differential-mode (DM) filter capacitor C_x and the filter components L_{CM} , C_{Y1} , and C_{Y2} are also shown in the model. The value of the stray capacitances C_{g1} , C_{g2} , C_{g3} , and C_{g4} of MOSFETs is very low compared with that of C_{PVg} ,

International Journal of Advanced Research in Electrical, Electronics and Instrumentation Engineering

(An ISO 3297: 2007 Certified Organization)

Vol. 5, Issue 4, April 2016

therefore the influence of these capacitors on the leakage current can be neglected. It is also noticed that the DM capacitor C_x does not affect the CM leakage current. Moreover, during the positive half-line cycle, switches S2, S4, and S6 are kept deactivated; hence the controlled voltage sources V_{2N} and V_{4N} are equal to zero and can be removed.

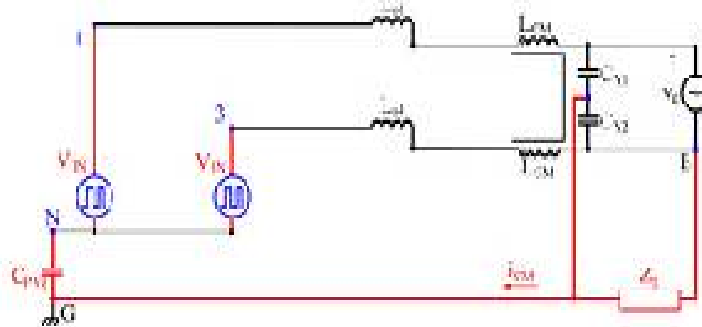


Fig.7 Simplified CM Leakage current analysis model for positive half cycle

A simplified CM leakage current model for the positive half-line cycle is derived in fig.7. a single-loop mode applicable to the CM leakage current analysis for the positive half-line cycle of the proposed transformerless inverter is obtained.

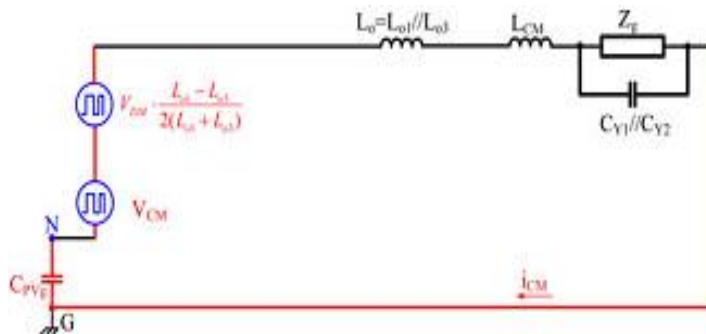


Fig.8 Simplified Single loop CM Leakage current analysis model for positive half cycle

Common mode voltage,

$$V_{CM} = \frac{V_{1N} + V_{3N}}{2} \quad (1)$$

Differential mode voltage,

$$V_{DM} = (V_{1N} - V_{3N}) \quad (2)$$

Total common mode voltage,

$$V_{iCM} = V_{CM} + V_{DM} \cdot \frac{L_{01} - L_{03}}{2(L_{01} + L_{03})}$$

$$V_{iCM} = \frac{V_{1N} + V_{3N}}{2} + (V_{1N} - V_{3N}) \cdot \frac{L_{01} - L_{03}}{2(L_{01} + L_{03})} = \frac{V_{dc}}{2} \quad (3)$$

It is clear that if the total CM voltage V_{iCM} keeps constant, no CM current flows through the converter. For a well-designed circuit with symmetrically structured, normally L_{01} is equal to L_{03} . During the active stage of the positive half-line cycle, V_{1N} is equal to V_{dc} , while V_{3N} is equal to 0. Similarly, during the whole negative half-line cycle, the CM

International Journal of Advanced Research in Electrical, Electronics and Instrumentation Engineering

(An ISO 3297: 2007 Certified Organization)

Vol. 5, Issue 4, April 2016

leakage current mode is exactly the same as the one during the positive half-line cycle; the only difference is the activation of different devices. The total CM voltage in the negative half-line cycle is also equal to $V_{dc}/2$.

V. SPECIFICATION AND POWER DEVICES

The specifications and power devices used for the proposed transformerless PV inverter are shown in Table 1. The switches used are superjunction MOSFET which improves the efficiency of the system.

Table 1. Specification and Power Devices

PARAMETERS	SPECIFICATION
Nominal input voltage	380V
Grid voltage	230VAC
Frequency	50HZ
AC current	21A
Switching frequency	20khz
Power devices S1-S6	IPW60R041C6
Diode D1-D6	APT30DQ60BG
L1,L2	0.96H
C_{PVg}	100nF
C_{Y1}, C_{Y2}	2.2nF
Output power	5KW

VI. MATLAB SIMULATION MODEL OF PROPOSED TRANSFORMERLESS INVERTER

The MATLAB Simulation model of Proposed Transformerless Inverter having 5 kW output power with 380V DC input voltage and 230V AC Grid voltage is as shown in Fig. 9.

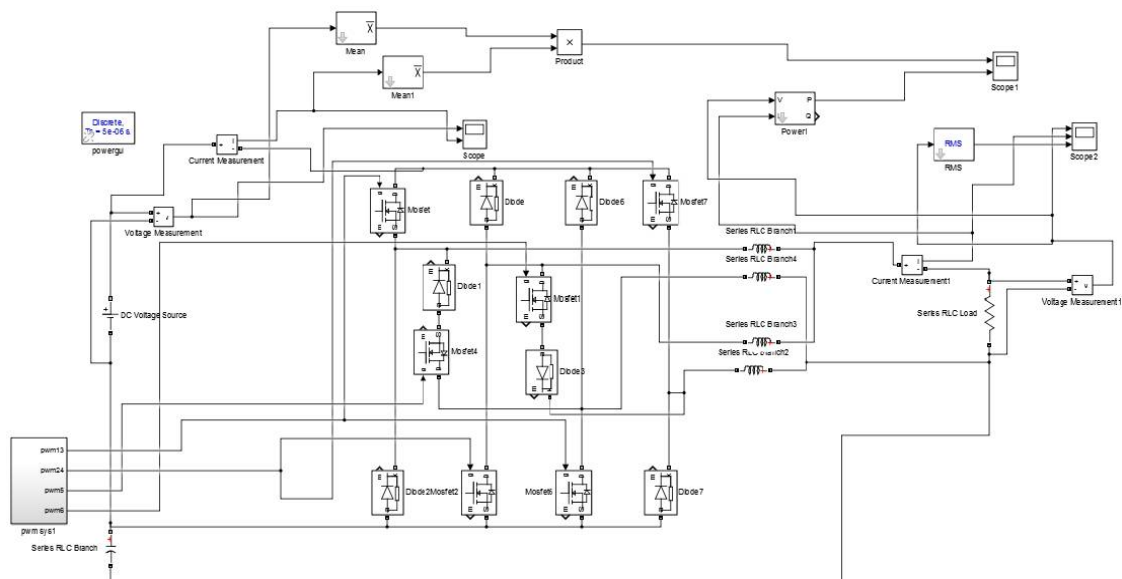


Fig. 9 Simulation Model of Proposed Transformerless Inverter

International Journal of Advanced Research in Electrical, Electronics and Instrumentation Engineering

(An ISO 3297: 2007 Certified Organization)

Vol. 5, Issue 4, April 2016

PWM for MOSFET S1,S3 and S2,S4 are produced by comparing Sine wave with half triangular wave as shown in fig.10.

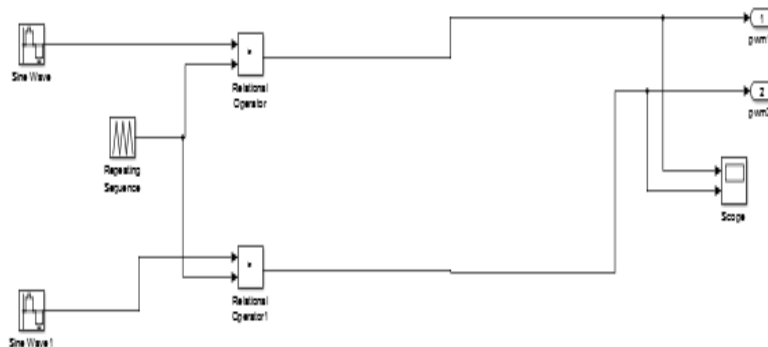


Fig.10 Simulation for PWM signal generation for S1, S3 and S2, S4

PWM at zero instant for freewheeling MOSFET S5 and S6 are generated as shown in Fig.11.

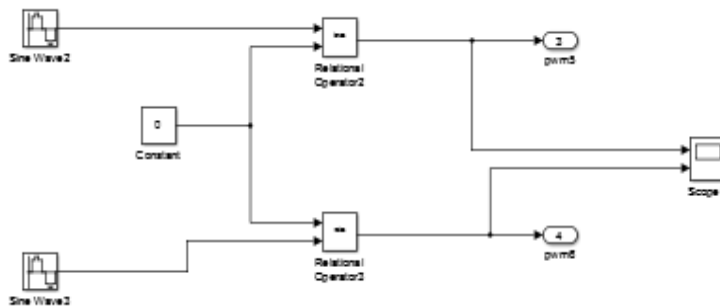


Fig.11 Simulation for PWM Signal Generation for S5 and S6

VII. SIMULATION RESULTS

Simulation result of Gate Signals for switches S1 to S6 is as shown in Fig.12 and Fig.13. Drain-source voltage waveform of grid current S5, S1 and S3 is in Fig.14.

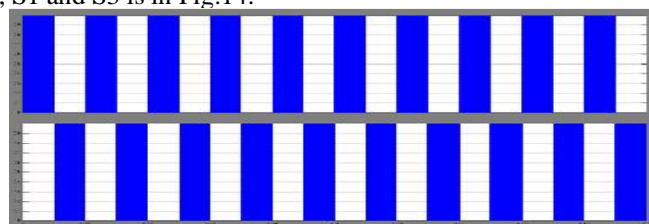


Fig.12 Gate signal of S1,S2 and S3,S4

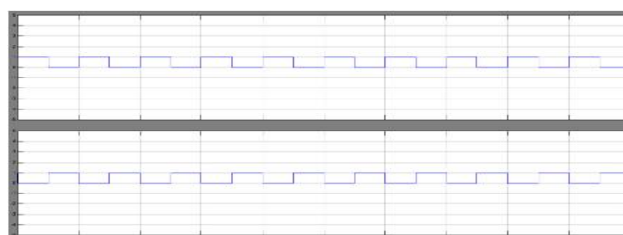


Fig.13 Gate signal of S5 and S6

International Journal of Advanced Research in Electrical, Electronics and Instrumentation Engineering

(An ISO 3297: 2007 Certified Organization)

Vol. 5, Issue 4, April 2016

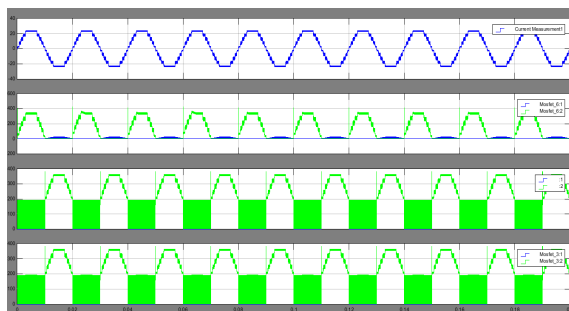


Fig.14 Drain-source voltage waveform of Grid current S5,S1 and S3

Input and output voltage and current waveform as shown in Fig. 15 and Fig. 16 are modeled for proposed inverter with 97% efficiency.

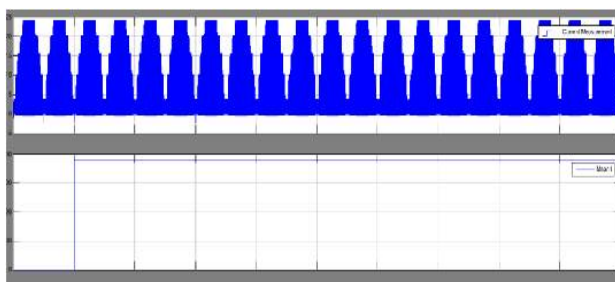


Fig.15 Input Voltage, Current and Power

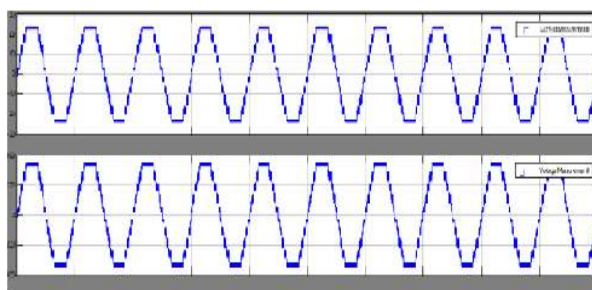


Fig.16 Output Voltage, Current and Power

VIII. CONCLUSION

In this paper study of conventional H5, H6 and Proposed transformerless inverter has been done. A high efficiency Proposed Transformerless Inverter for PV grid-connected power generation systems is simulated and corresponding simulation results are presented. The main characteristics of the proposed transformerless inverter are summarized as follows:

1. High efficiency can be achieved by employing super junction MOSFETs for all switches since their body diodes are never activated.
2. CM leakage current is reduced due to two additional unidirectional current switches (S5 and S6) which decouple the PV array from the grid during the zero stages.
3. For high inverter efficiency, higher switching frequency (20 KHz) operation is allowed to reduce the output current ripple and the size of passive components.



ISSN (Print) : 2320 – 3765
ISSN (Online): 2278 – 8875

International Journal of Advanced Research in Electrical, Electronics and Instrumentation Engineering

(An ISO 3297: 2007 Certified Organization)

Vol. 5, Issue 4, April 2016

REFERENCES

- [1] Bin Gu, Jason Dominic, Jih-Sheng Lai, Chien-Liang Chen, Thomas LaBella, and Baifeng Chen, “High Reliability and Efficiency Single-Phase Transformerless Inverter for Grid-Connected Photovoltaic Systems”; IEEE transactions on power electronics, Vol. 28, no. 5, pp.2235-2245, May 2013.
- [2] Baifeng Chen, Bin Gu, Lanhua Zhang, Zaka Ullah Zahid, Jih-Sheng (Jason) Lai, Zhiling Liao, and Ruixiang Hao, “A High-Efficiency MOSFET Transformerless Inverter for Nonisolated Microinverter Applications”; IEEE transactions on power electronics, Vol. 30, no. 7, pp.3610-3622, July 2015.
- [3] Wuhua Li, Yunjie Gu, Haoze Luo, Wenfeng Cui, Xiangning, “Topology Review and Derivation Methodology of Single-Phase Transformerless Photovoltaic Inverters for Leakage Current Suppression” IEEE transactions on industrial electronics, Vol. 62, no. 7, pp.4537-4551, July 2015.
- [4] Oscar Lopez, Francisco D. Freijedo, Alejandro G. Yepes, Pablo Fernandez-Comesana, Jano Malvar, Remus Teodorescu and Jesus Doval-Gandoy, “Eliminating Ground Current in a Transformerless Photovoltaic Application”, IEEE transactions on energy conversion, Vol. 25, no. 1, pp. 140-147, Mar. 2010.